

Critical surface coupling in anisotropic Heisenberg ferromagnets

J. N. B. de Moraes and W. Figueiredo

Departamento de Física, Universidade Federal de Santa Catarina, 88049 Florianópolis, Santa Catarina, Brazil

(Received 22 February 1991; revised manuscript received 29 July 1991)

We consider an anisotropic Heisenberg model on a semi-infinite cubic lattice within the Green-function formalism. We analyze various possible configurations for the surface and bulk anisotropy parameters. We determine a complete phase diagram for the multicritical points and our results are in agreement with real-space renormalization-group calculations.

I. INTRODUCTION

Surface magnetism has been a subject of growing interest in the recent years. From a theoretical point of view, several techniques have been used to investigate surface magnetic ordering: effective-field theories,^{1,2} series expansions,³ Monte Carlo simulations,^{4,5} renormalization-group techniques,⁶⁻⁸ and Green functions.⁹⁻¹¹

Since the discovery¹² in 1981 that Gd can exhibit a magnetically ordered phase over a magnetically disordered bulk, techniques have been devised to probe the magnetization of the surface layers. Among these, the most frequently used is the spin-polarized low-energy electron diffraction (SPLEED).^{13,14} For a discussion of these experimental methods, we refer to the paper of Celotta and Pierce.¹⁵

In this paper we consider an anisotropic Heisenberg model on a semi-infinite cubic lattice. Through a suitable choice of the anisotropy parameters of the volume and surface, we can determine different configurations for the spin ordering of the system. We apply to this problem the Green-function formalism with a random-phase approximation (RPA). This method is particularly interesting because we obtain the magnetization profile and dispersion relations for the surface spin waves as a function of temperature. We determine a complete phase diagram of multicritical points as a function of the anisotropy parameters. In particular, we discuss the delicate point about the sums inside the first Brillouin zone, in the case where the surface and volume are both described by pure Heisenberg models.

In Sec. II we present the model Hamiltonian and calculations performed using the Green-function formalism. In Sec. III we present the results and discussions for the magnetization profile and phase diagram of our model. Finally, in Sec. IV we present our conclusions.

II. DESCRIPTION OF THE MODEL AND CALCULATIONS

We consider the following model Hamiltonian on a semi-infinite simple-cubic lattice:

$$H = - \sum_{\langle i,j \rangle} [J_{ij}(1 - \epsilon_{ij})(S_i^x S_j^x + S_i^y S_j^y) + J_{ij} S_i^z S_j^z], \quad (1)$$

where J_{ij} represents the exchange interaction between all pairs $\langle ij \rangle$ of nearest-neighboring spins. We choose the following values for the parameters J_{ij} and ϵ_{ij} : If the sites i and j are at the surface plane ($l=0$), we take $J_{ij}=J_s$ and $\epsilon_{ij}=\epsilon_s$; if i is at the surface plane ($l=0$) and j is at the next inner plane ($l=1$), we take $J_{ij}=J_\perp$ and $\epsilon_{ij}=\epsilon_\perp$. For all others neighboring sites, $J_{ij}=J$ and $\epsilon_{ij}=\epsilon$. The $S_i^{x,y,z}$ are the components of the spin- $\frac{1}{2}$ operators. If $\epsilon=0$, we have a Heisenberg model, while the value $\epsilon=1$ represents an Ising model. In our calculations based on the Green-function formalism, we must avoid the value $\epsilon=1$. Therefore, we will take in our analysis the value $\epsilon=0.99$ as representing the limit to the Ising model. We can see that by choosing the values of the parameters ϵ_s and ϵ between zero and 1 we obtain different combinations of models between the surface and bulk. The surface is parallel to the (010) plane, and we assume that the spins will be oriented preferentially parallel to the surface, so that demagnetizing fields can be neglected.

The equations of motion for the Fourier transform of the Green functions $\langle\langle S_i^+(t); S_m^-(t') \rangle\rangle$, are given by

$$\begin{aligned} \left[E - \sum_i J_{il} \langle S_i^z \rangle \right] \langle\langle S_i^+; S_m^- \rangle\rangle_E \\ + \langle S_i^z \rangle \sum_i (1 - \epsilon_{il}) J_{il} \langle\langle S_i^+; S_m^- \rangle\rangle_E = \frac{1}{\pi} \langle S_i^z \rangle \delta_{lm}, \end{aligned} \quad (2)$$

where $\langle\langle S_i^+; S_m^- \rangle\rangle_E$ are the Fourier transforms of the Green functions and we have employed the RPA decoupling. In our calculations we have assumed that the mean value $\langle S_i^z \rangle$ is the same for all sites in a given plane l , that is,

$$\langle S_i^z \rangle = \langle S_l^z \rangle, \quad (3)$$

where $l=0$ is the surface plane, $l=1$, the next inner plane, and so on. For $l \geq 2$ we have also taken $\langle S_l^z \rangle = \langle S^z \rangle_b$, where $\langle S^z \rangle_b$ stands for the bulk magnetization per site.

Because of translational symmetry parallel to the surface plane, we introduce the Fourier transform of the Green functions, $G(\mathbf{K}, E)$, where the wave vectors \mathbf{K} belong to the two-dimensional Brillouin zone of a square

lattice. After some tedious manipulations, the Green functions can be determined by the following matrix equation:

$$[\underline{\Omega} \underline{G}]_{lm} = \frac{1}{\pi} \langle S_l^z \rangle \delta_{lm}, \quad (4)$$

where $\underline{\Omega}$ is given by

$$\underline{\Omega} = \begin{pmatrix} 2t + \alpha_{00} & \Omega_{01} & 0 & 0 & 0 & 0 & \cdots \\ \Omega_{10} & 2t + \alpha_{11} & \Omega_{12} & 0 & 0 & 0 & \cdots \\ 0 & \alpha & 2t + \alpha_{22} & \alpha & 0 & 0 & \cdots \\ 0 & 0 & \alpha & 2t & \alpha & 0 & \cdots \\ \vdots & \vdots & 0 & \alpha & 2t & \alpha & \cdots \end{pmatrix}, \quad (5)$$

and we have defined that

$$\alpha_{00} = [(1 - \epsilon_s) J_s z \gamma_{\mathbf{K}} - z J_s] \langle S_0^z \rangle - J_{\perp} \langle S_1^z \rangle - [z(1 - \epsilon) J \gamma_{\mathbf{K}} - (2 + z) J] \langle S_2^z \rangle, \quad (6)$$

$$\alpha_{11} = -J_{\perp} \langle S_0^z \rangle + [(1 - \epsilon) J z \gamma_{\mathbf{K}} - z J] \langle S_1^z \rangle - [z(1 - \epsilon) J \gamma_{\mathbf{K}} - (1 + z) \epsilon J] \langle S_2^z \rangle, \quad (7)$$

$$\alpha_{22} = -\epsilon J \langle S_1^z \rangle + \epsilon J \langle S_2^z \rangle, \quad (8)$$

$$\Omega_{01} = (1 - \epsilon_1) J_{\perp} \langle S_0^z \rangle, \quad (9)$$

$$\Omega_{10} = (1 - \epsilon_1) J_{\perp} \langle S_1^z \rangle, \quad (10)$$

$$\Omega_{12} = (1 - \epsilon) J \langle S_1^z \rangle, \quad (11)$$

$$\alpha = (1 - \epsilon) J \langle S_2^z \rangle, \quad (12)$$

$$2t = \{E + [z(1 - \epsilon) J \gamma_{\mathbf{K}} - (2 + z) J]\} \langle S_2^z \rangle. \quad (13)$$

In the above equations, $\gamma_{\mathbf{K}} = \frac{1}{2} [\cos(aK_x) + \cos(aK_z)]$ is the structure factor for a square lattice ($z=4$) of spacing a . In order to determine the layer magnetization, we need to calculate the matrix elements of $\underline{\Omega}^{-1}$. It is straightforward to show that

$$(\underline{\Omega}^{-1})_{ll} = \frac{N_l(\xi)}{D(\xi)}, \quad (14)$$

where

$$N_0(\xi) = \xi [\alpha_{22} \xi^3 + (\alpha^2 - \alpha \Omega_{12} + \alpha_{11} \alpha_{22}) \xi^2 + \alpha^2 (\alpha_{11} + \alpha_{22}) \xi + \alpha^4], \quad (15)$$

$$N_1(\xi) = \xi [\alpha_{22} \xi^3 + (\alpha^2 + \alpha_{00} \alpha_{22}) \xi^2 + \alpha^2 (\alpha_{00} + \alpha_{22}) \xi + \alpha^4], \quad (16)$$

and

$$D(\xi) = \sum_{i=0}^5 a_i \xi^i, \quad (17)$$

with

$$a_0 = \alpha^6, \quad (18)$$

$$a_1 = \alpha^4 (\alpha_{00} + \alpha_{11} + \alpha_{22}), \quad (19)$$

$$a_2 = 2\alpha^4 - \Omega_{12} \alpha^3 + (\alpha_{11} + \alpha_{22}) \alpha_{00} + \alpha_{11} \alpha_{22} - \Omega_{01} \Omega_{10}, \quad (20)$$

$$a_3 = (\alpha_{00} + \alpha_{11} + \alpha_{22}) \alpha^2 - \alpha_{00} \Omega_{12} \alpha - \alpha_{22} \Omega_{01} \Omega_{10} + \alpha_{00} \alpha_{11} \alpha_{22}, \quad (21)$$

$$a_4 = \alpha^2 - \Omega_{12} \alpha + (\alpha_{00} + \alpha_{11}) \alpha_{22}, \quad (22)$$

$$a_5 = \alpha_{22}. \quad (23)$$

The parameter ξ is given by the solution of the equation

$$\xi^2 - 2t\xi + \alpha^2 = 0. \quad (24)$$

The roots of the above equation are complex for $|t| < \alpha$. In this case we can write that $t = -\alpha \cos(aK_y)$, and if we put this in Eq. (13), we recover the bulk dispersion relation for magnons. On the other hand, if $|t| > \alpha$, the roots of Eq. (24) are real and only those for which $|\xi| < 1$ will have a physical meaning. As we can see from Eqs. (4) and (14), the poles of the Green functions are given by the real roots of the equation

$$D(\xi_s) = 0. \quad (25)$$

The spectrum of the surface magnons can be obtained from the roots of the above equation with the restriction that $|\xi_s| < 1$. Then we have the following expression for the surface magnons:

$$\nu_{\mathbf{K}} = (\xi_s - \alpha^2 \xi_s^{-1}) - [(1 - \epsilon) z J \gamma_{\mathbf{K}} - (2 + z) J] \langle S_2^z \rangle. \quad (26)$$

Nevertheless, in order to calculate the roots of $D(\xi_s)$, it is necessary to evaluate the layer magnetizations $\langle S_0^z \rangle$ and $\langle S_1^z \rangle$ and the bulk magnetization $\langle S^z \rangle_b$, which in our approximation is attained at the third layer. Therefore, from the properties of the Green functions,¹⁶ we can show that

$$\langle S_{0,1}^z \rangle = \frac{\frac{1}{2}}{1 + 2\phi_{0,1}}, \quad (27)$$

where

$$\phi_{0,1} = -\frac{2}{\pi} \left[\frac{a}{2\pi} \right]^2 \int d\mathbf{K} \left[\int_{-\alpha}^{\alpha} dt \frac{\text{Im}[N_{0,1}(\xi)/D(\xi)]}{(e^{\beta\nu} - 1)} + \frac{\pi}{2} \sum_{\gamma} \frac{N_{0,1}(\xi_{\gamma})}{D'(\xi_{\gamma})} \frac{(\alpha^2 - \xi_{\gamma}^2)}{\xi_{\gamma}^2 (e^{\beta\nu} - 1)} \right], \quad (28)$$

ξ_{γ} being the real roots of $D(\xi_{\gamma})$ and $D'(\xi_{\gamma})$ its derivative calculated at the point $\xi = \xi_{\gamma}$. The energy spectrum is given by

$$\nu = 2t - [(1 - \epsilon) z J \gamma_{\mathbf{K}} - (2 + z) J] \langle S^z \rangle_b, \quad (29)$$

$\beta = (k_B T)^{-1}$, k_B is the Boltzmann constant, and T is the absolute temperature.

In our calculations we first must determine the bulk magnetization as a function of temperature. It is easy to show that

$$\langle S^z \rangle_b = \frac{\frac{1}{2}}{1+2\phi}, \quad (30)$$

where

$$\phi = \frac{1}{N} \sum_{\mathbf{q}} (e^{\beta\omega_{\mathbf{q}}} - 1)^{-1}, \quad (31)$$

and

$$\omega_{\mathbf{q}} = zJ \langle S^z \rangle_b [1 - (1 - \epsilon)\Gamma_{\mathbf{q}}] \quad (32)$$

is the spectrum of the bulk magnons. Here the \mathbf{q} values run over the first Brillouin zone of a simple cubic lattice ($z = 6$) with structure factor $\Gamma_{\mathbf{q}}$. The sum in Eq. (31) was performed using a set of 816 special points in the first zone that can be obtained from the work of Chadi and Cohen.¹⁷

The set of equations (27)–(29) must be solved self-consistently for $\langle S_0^z \rangle$ and $\langle S_1^z \rangle$ for each value of temperature. In this way we are able to determine the bulk magnetization and the first- and second-layer magnetizations, as well as the spectrum of the bulk and surface magnons for our semi-infinite anisotropic Heisenberg model, as functions of temperature.

The above formalism is suitable for temperatures below the bulk critical temperature. As we are also interested in situations where we can have a surface magnetic order over a paramagnetic bulk, we must consider this case separately. If we put $\langle S^z \rangle_b = 0$, for $l \geq 2$, in our system of equations (2), the matrix Ω becomes simpler and the calculations follow along the same lines as before. We do not present here the explicit expressions for the layer magnetization and magnon surface spectrum.

III. RESULTS

We present in Fig. 1 the curves of magnetization of the two first layers and bulk as a function of temperature for $\epsilon_s = 0.0$, $\epsilon = 0.89$, $J_s/J = 2.78$. In this case the bulk is described by an anisotropic Heisenberg model, while at the surface we have a pure Heisenberg model. For these

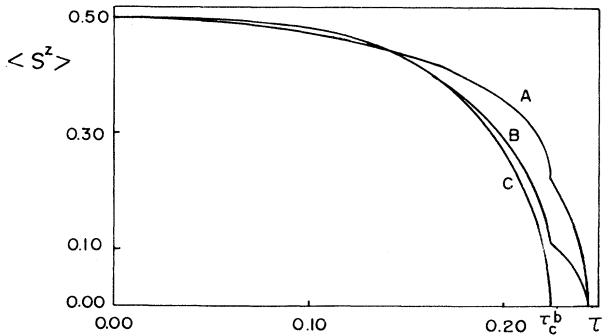


FIG. 1. Magnetization as a function of the reduced temperature ($\tau = k_B T/6J$). A, B, and C represent the first layer, second layer, and bulk magnetization, respectively. We have $\epsilon_s = 0$, $\epsilon = 0.89$, $J_s/J = 2.78$, $\epsilon_1 = \epsilon$, and $J_1/J = 1.0$. τ_c^b is the bulk critical temperature.

values of the parameters, our model exhibits a surface ordering above the paramagnetic bulk critical temperature (τ_c^b) and the slope of the magnetization curves of the first two layers is discontinuous. This is also supported by renormalization-group calculations.^{7,8} On the other hand, recent Monte Carlo calculations⁵ give a continuous slope at (τ_c^b). Moran-Lopes and Sanches² have shown, within a mean-field approximation, that the discontinuity in the derivative is due to the limited number of independent planes above the bulk.

Increasing the number of independent planes, the discontinuity disappears. From an experimental point of view, measurements¹⁸ on Gd show no discontinuous slope in the magnetization curve at the bulk critical temperature. We believe that the observed discontinuity in the slope of the magnetization at (τ_c^b) is due to our approximation, in which the third plane is taken as the bulk plane.

In Fig. 2 we have plotted the surface critical temperature ($\tau_c^s = k_B T/6J$) as a function of J_s/J . This phase diagram exhibits three distinct phases, namely, the paramagnetic (P), surface ferromagnetic (SF), and bulk ferromagnetic (BF). They meet at the multicritical point, which occurs for $(J_s/J)_c = 2.27$, when $\epsilon_s = 0.00$ and $\epsilon = 0.89$. The value of $(J_s/J)_c$ is defined as the particular value of J_s/J , above which we can have surface ordering even for a paramagnetic bulk. For the values of J_s/J less than $(J_s/J)_c$, the bulk and surface order at the same critical temperature.

We observe in Fig. 3 the behavior of the relative surface critical temperature as a function of ϵ_s , when $\epsilon = 0.89$. We have chosen to plot the different curves for constant values of $[(2 - \epsilon_s)/(2 - \epsilon)](J_s/J)$ because they become almost straight lines. For the values of J_s/J greater than $(J_s/J)_c = 2.27$, the surface can always be ordered over a paramagnetic bulk. On the other hand, for $(J_s/J) \leq 2.27$, the surface can order only above a given value of the surface anisotropy parameter ϵ_s .

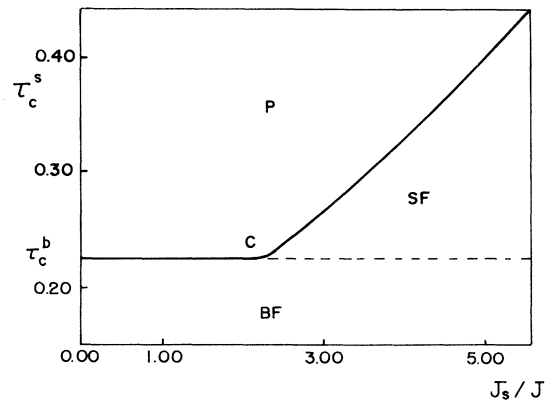


FIG. 2. Surface critical temperature (τ_c^s) as a function of the relative coupling J_s/J . BF, SF, and P, respectively, represent the bulk ferromagnetic, surface ferromagnetic, and paramagnetic phases. We have $\epsilon_s = 0$, $\epsilon = 0.89$, $\tau_c^s = k_B T/6J$, $\epsilon_1 = \epsilon$, and $J_1/J = 1.0$; C denotes the multicritical point.

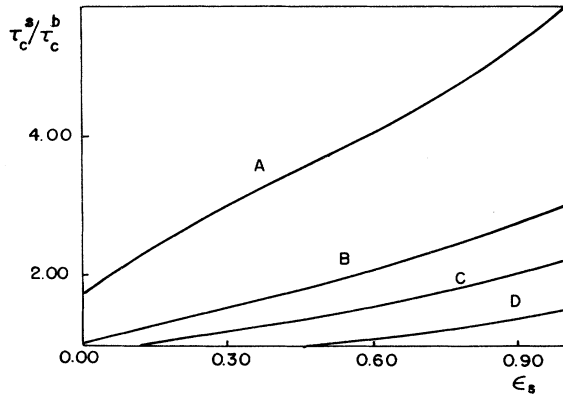


FIG. 3. Relative critical surface temperature (τ_c^s/τ_c^b) as a function of the surface anisotropy parameter (ϵ_s). We have $\epsilon=0.89$, $(J_s/J)_c=2.27$, $\epsilon_1=\epsilon$, and $J_1/J=1.0$. Curves are for constant values of $RJ=[(2-\epsilon_s)/(2-\epsilon)](J_s/J)$. A ($RJ=8.0$), B ($RJ=4.09$), C ($RJ=3.0$), and D ($RJ=2.0$).

Finally, we exhibit in Fig. 4 the location of the multicritical points where all three P -BF, P -SF, and BF-SF critical lines join, that is, for a given pair of values of ϵ_s and ϵ , the value of $(J_s/J)_c$ above which the surface ferromagnetic phase appears. Our diagram, obtained within Green-function formalism, is similar to that obtained by Mariz, Costa, and Tsallis⁷ through a real-space renormalization-group calculation.

We point out that with the use of Green-function techniques it is not possible to obtain exactly the condition ϵ_s or $\epsilon=1$, which would represent an Ising model. In our calculations we take ϵ_s or $\epsilon=0.99$ as representing the Ising model behavior. In particular, if $\epsilon_s=\epsilon=0.99$ (surface and bulk quasi-Ising), a critical value $(J_s/J)_c=1.37$ is obtained. The value found by Mariz, Costa, and Tsallis⁷ was 1.74. Results from a mean-field approximation give the value 1.25, while series expansions³ give 1.6 and a Monte Carlo simulation⁴ gives 1.5. When $\epsilon_s=0$ (surface Heisenberg), we observe that the critical line decreases smoothly from $\epsilon=1.00$, exhibits a minimum at $\epsilon=0.058$, with $(J_s/J)_c=2.21$, and then begins to increase, showing a divergent behavior at $\epsilon=0.0$.

We now focus our attention to the region of the diagram in which the surface and bulk are both described by Heisenberg models. We can see that all critical lines present a divergent behavior when we approach this region. It is interesting to note that this behavior, obtained through the use of the Green-function method with the RPA approximation, is similar to that obtained previously with the use of the renormalization group.⁷ In that paper the authors suggest that with Green functions within the RPA it is not possible to obtain a divergent behavior. We now explain why we are able to determine a divergent behavior. When we work with the Green-function formalism, usually, we must perform sums over wave vectors in the first Brillouin zone. In our case we can use a small number of two-dimensional special points,¹⁹ which are points of high symmetry in the first Brillouin zone. With these few points the computational efforts are greatly reduced. Nevertheless, we must use these points with

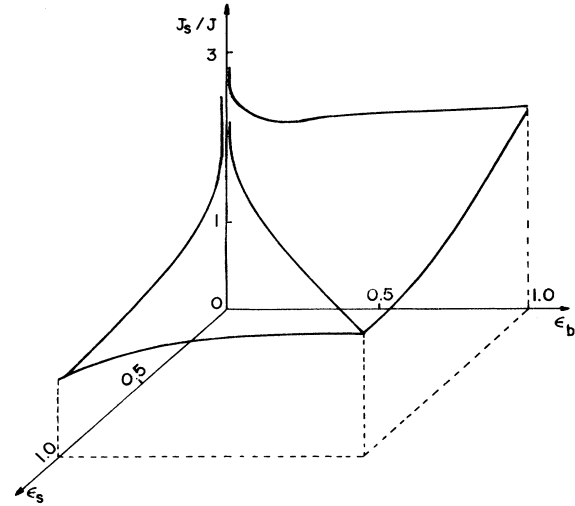


FIG. 4. Critical coupling (J_s/J) as a function of the surface (ϵ_s) and bulk (ϵ) anisotropy parameters. The critical lines locate the multicritical points.

caution when the surface is described by a Heisenberg model. In this case the spectrum of magnons goes as K^2 in the neighborhood of $\mathbf{K}=0$, and the integrals over \mathbf{K} [Eq. (28)] need to take into account these contributions. For example, using the ten special points of Cunningham,¹⁹ the nearest special point of $\mathbf{K}=0$ is $\mathbf{K}=(\pi/8a, \pi/8a)$, and the contribution to the integral is not very important. As a consequence, we find a finite critical value for $(J_s/J)_c$; that is, the surface can order over a paramagnetic bulk, even when surface and bulk are both described by pure Heisenberg models.

But if we divide the first Brillouin zone in a fine net of points, the contribution around the center of the Brillouin zone becomes more realistic. With this in mind we performed the sum using up to 2×10^6 points on an IBM 3090 computer. The results are quite surprising: The values of $(J_s/J)_c$ seem to go to infinity when we increase the number of points in the first Brillouin zone. Therefore, as in the renormalization-group calculations, the Green-function method asserts that the surface cannot order over a paramagnetic bulk when surface and bulk are both represented by pure Heisenberg models.

IV. CONCLUSIONS

We have considered in this work the application of the method of Green functions to the study of the phase transitions in a semi-infinite anisotropic Heisenberg model. Through a suitable choice of anisotropy parameters, we could determine the complete phase diagram in the space of the critical coupling and anisotropy parameters of the surface and bulk. Our phase diagram for the multicritical points, where a bulk ferromagnetic, surface ferromagnetic, and a paramagnetic phase join, is in agreement with earlier results obtained via real-space renormalization-group calculations. The discontinuity that appears in the slope of the magnetization curve at

the bulk critical temperature may be a consequence of the limited number of independent planes used in our calculations. An increase in the number of independent planes would take a much longer time of computation, but the results would change slightly. For instance, when the number of perturbed planes varies from two to three, the surface critical temperature increases only 1%. Meanwhile, we cannot say anything about the number of perturbed independent planes necessary to suppress the discontinuity in the slope of the magnetization at the bulk critical temperature. On the other hand, as RPA decoupling is equivalent to the mean-field approximation in the vicinity of the critical points, we expect that the discontinuity in the slope of the magnetization disappears as we increase the number of independent planes.

We have also explained why we were able to observe

no finite critical coupling when surface and bulk are both described by pure Heisenberg models. The use of a small number of special points in the first Brillouin zone causes a finite critical coupling because we cannot approach sufficiently close to the center of the Brillouin zone. Nevertheless, by using a huge number of points, the divergent critical behavior appears naturally.

ACKNOWLEDGMENTS

This work was partly supported by the Brazilian Agencies Conselho Nacional de Desenvolvimento Científico e Tecnológico (CNPq) and Financiadora de Estudos e Projetos (FINEP). We also acknowledge Dr. Silvia Selzer and Dr. Norberto Majlis for many suggestions and Dr. Jürgen F. Stilck for a critical reading of the manuscript.

¹D. L. Mills, Phys. Rev. B **3**, 3887 (1971).

²J. L. Moran-Lopes and J. M. Sanchez, Phys. Rev. B **39**, 9746 (1989).

³K. Binder and P. C. Hohenberg, Phys. Rev. B **9**, 2194 (1971).

⁴K. Binder and D. P. Landau, Phys. Rev. Lett. **52**, 318 (1984).

⁵D. P. Landau and K. Binder, Phys. Rev. B **41**, 4786 (1990).

⁶S. Dietrich and E. Eisenriegler, Phys. Rev. B **27**, 2937 (1983).

⁷A. M. Mariz, U. M. S. Costa, and C. Tsallis, Europhys. Lett. **3**, 27 (1987).

⁸K. Ohno and Y. Okabe, Phys. Rev. B **39**, 9764 (1989).

⁹S. Selzer and N. Majlis, Phys. Rev. B **27**, 544 (1983).

¹⁰Y. Endo and T. Ayukawa, J. Phys. Soc. Jpn. **58**, 2515 (1989).

¹¹C. A. Queiroz and W. Figueiredo, Phys. Rev. B **40**, 4967 (1989).

¹²C. Rau and S. Eichner, in *Nuclear Methods in Materials Research*, edited by K. Bethge, H. Bauman, H. Jex, and F. Rauch (Vieweg, Braunschweig, 1980), p. 354.

¹³D. Weller, S. F. Alvarado, W. Gudat, K. Schröder, and M. Campagna, Phys. Rev. Lett. **14**, 1555 (1985).

¹⁴W. Dürr, M. Taborelli, O. Paul, R. Germar, W. Gudat, D. Pescia, and M. Landolt, Phys. Rev. Lett. **62**, 206 (1989).

¹⁵R. J. Celotta and D. T. Pierce, Science **234**, 249 (1986).

¹⁶D. N. Zubarev, Usp. Fiz. Nauk **71**, 71 (1971) [*Sov. Phys. Usp.* **3**, 320 (1960)].

¹⁷D. J. Chadi and M. L. Cohen, Phys. Rev. B **8**, 5747 (1973).

¹⁸C. Rau and M. Robert, Phys. Rev. Lett. **58**, 2714 (1987).

¹⁹S. B. L. Cunningham, Phys. Rev. B **10**, 4988 (1974).